

Mesoscale Quantization and Self-Organized Stability

Randall D. Peters
Mercer University Physics

June 2005

Abstract

In the world of technology, one of the most important forms of friction is that of rolling friction. Yet it is one of the least studied of all the known forms of energy dissipation. In the present experiments we investigate the oscillatory free-decay of a rigid cube, whose side-length is less than the diameter of the rigid cylinder on which it rests. The resulting free-decay is one of harmonic motion with damping. The non-dissipative character of the oscillation yields to a linear differential equation; however, the damping is found to involve more than a deterministic nonlinearity. Dominated by rolling friction, the damping is sensitive to the material properties of the contact surfaces. For 'clean' surfaces of glass on glass, the decay shows features of mesoscale quantization and self-organized stability.

1 Geometry

Shown in cross-section in figure 1 are the two objects that comprise this oscillatory system. The cube side-length dimension is $2a$, and the diameter of the cylinder is $2r$. Both are assumed to be completely rigid, so that the torque which restores the cube toward equilibrium is due to gravity. In mechanics textbooks this problem is commonly treated as an exercise to test for the condition of static equilibrium.

2 Theory without damping

The potential energy is simply mgh . From the other identities provided in the figure, one can readily show for small displacements, that

$$U = \frac{mg}{2}(r-a)\theta^2 \quad (1)$$

The displacement of the center of mass P of the cube is given by $\Delta x = r \sin \theta - s \sin(\phi - \theta)$, $\Delta y = s \cos(\phi - \theta) - a$. For small θ these yield for the center of mass velocity

$$v_x \rightarrow a \frac{d\theta}{dt} = a\dot{\theta}, \quad v_y \rightarrow 0 \quad (2)$$

The moment of inertia of the cube about its center of mass is given by $I = \frac{2}{3}ma^2$. The kinetic energy is the sum of translational and rotational parts; i.e., $T = \frac{1}{2}mv^2 + \frac{1}{2}I\dot{\theta}^2 = \frac{5}{6}ma^2\dot{\theta}^2$. Using $p = \frac{\partial T}{\partial \dot{\theta}}$ the Hamiltonian is calculated to be

$$H(p, \theta) = \frac{3p^2}{10 ma^2} + \frac{mg}{2}(r-a)\theta^2 \quad (3)$$

Using Hamilton's canonical equations, $\frac{\partial H}{\partial p} = \dot{\theta}$ and $\frac{\partial H}{\partial \theta} = -\dot{p}$ one obtains the equation of motion

$$\ddot{\theta} + \frac{3g}{5a^2}(r-a)\theta = 0 \quad (4)$$

from which the period is determined to be

$$T = 2\pi\sqrt{\frac{5a^2}{3g(r-a)}} \quad (5)$$

3 Adding friction to the model

The naive approach to the addition of damping would be to add to the left hand side of eq.(4) the term $2\beta\dot{\theta}$, where β is sometimes referred to as the damping constant. In reality, in dozens of experiments performed by the present author on mechanical oscillators– not a single case has ever been found for which it is proper to call β a constant. Even if the present system were amenable to the overly-idealized viscous damping approximation indicated by this term, β is never constant and should be referred to as the viscous damping *coefficient*. With fluids it depends on the density as well as the viscosity, and it is never completely independent of frequency[1].

3.1 Nonlinear damping

From the experimental results it will be seen that the damping is certainly not a classical exponential decay of the type students are conditioned from their textbooks to expect for virtually every oscillatory system in free-decay. A closer approximation to most of the cases (although inadequate) is ‘simple’ Coulomb damping; i.e., where one adds to eq.(4) a term that is proportional to $sgn(\dot{\theta})$. The signum function causes the effective damping force to depend on the direction of the velocity but not its magnitude. It is a nonlinear damping term, and the quality factor Q decreases linearly with time, as opposed to being constant [1].

4 Experimental Setup

Shown in figure 2 is a photograph of the apparatus that was employed for this study. The material of both cylinder and cube is glass, components normally used for optics experiments. All surfaces are highly polished, so that visible light is specularly reflected from them. The dimensions are $r = 4.46\text{ cm}$, & $a = 2.54\text{ cm}$. The thin half-cylinder (length = 1.4 cm) is glued at its bottom to the aluminum block on which it rests. The block is in turn glued to the wooden base to which the sensor support ‘post’ is attached with a screw.

Visible in the picture is a thin rectangular piece of sheet copper that was superglued to one side of the cube. Passing between static electrodes, it is the moving member of the capacitive sensor that was used to measure the displacement of the cube. The sensor is the symmetric differential capacitive (SDC) device invented and patented by the author[2].

The interface to the computer is a Dataq Inc. DI-154 analog to digital 12-bit converter. It was used instead of their \$25 10-bit DI-194 to permit lower-level signals to be studied. The 10-bit ADC would be satisfactory for many of the cases considered, with the SDC electronics set at maximum gain.

5 Experimental Results

5.1 Frequency

As a test of eq(5), the period of oscillation was measured using the Fast Fourier Transform (FFT) of free-decay records. A low-level case is shown in the right hand graph of figure 3. The second harmonic is down 33 dB (factor of 45) from the fundamental. It is not known whether this harmonic distortion results primarily from the sensor or if it is a characteristic of the cube/cylinder oscillator. It should be noted that the decibel, as used in all graphs (excepting figure 5), is according to the Dataq convention; i.e.,

$$dB = 20 \log_{10}(32768 v/v_{fs}) \quad (6)$$

where the full-scale voltage is for the present ADC not adjustable; i.e., it is fixed at $v_{fs} = 10 V$. Of course, as with potential energies, only differences are important; making the reference inconsequential. To convert to the more common dB relative to 1 volt, one only needs to subtract 70.3 from the Dataq dB value.

All spectra, both low-level and high-level, yielded the same 2.2 Hz eigenfrequency. With the dimensions indicated above, the theoretical estimate of the frequency from eq (5) is $f = \frac{1}{T} = 2.1 Hz$. This agreement to within 5% is considered reasonable, since the ‘regularity’ of the cylinder is unknown. Although the cube is polished flat to approximately the wavelength of visible light; variability in curvature around the cylinder as a function of angle is expected to be more significant.

It should be noted that the moment of inertia of the copper strip, which is not factored into the theory, will lower the frequency only slightly; since its mass is less than 2% the cube’s mass of 329 g.

Although the compressibility of the surfaces has not been considered in a quantitative manner, this may be important for efforts directed at better than 5% agreement between theory and experiment. The weight of the cube flattening the cylinder and cupping the cube at the contact point, causes the frequency to increase.

5.2 Damping

As can be seen from the compressed-time record of figure 3, the free-decay is not exponential. Moreover, it is not even symmetric; i.e., the upper and lower turning points of the motion are not mirror-symmetric about the time-axis.

At low levels of the motion, where the cube’s resting position on the cylinder can be maintained nearly constant, repeatability between runs was found to be good, as seen in the example of figure 4. To initialize the oscillation at these low levels, a stream of air was directed onto a side of the cube (a strong puff from the mouth). At high levels the oscillation was accomplished by placing a screwdriver under one side of the wooden base, tilting it by a small angle and then removing the tilt rapidly (but not by dropping).

The nonlinearities observed in figure 4 derive from the oscillator and not from the sensor. The sensor was determined to be essentially linear over the full operating range of plus and minus voltages considered in the study. The sensor was calibrated using an optical lever; i.e., by means of a laser pointer directed onto one surface of the cube (using a screen with a meter stick placed 3.6 m away). The calibration constant was measured to be 48 V/rad.

Damping Theory

Figure 5 illustrates the differences among hysteretic, Coulomb, and amplitude dependent damping. Hysteretic damping yields an exponential free-decay and may be approximated (for fixed frequency) by the viscous damping model. In actuality, all three of the damping cases shown in figure 5 are nonlinear. Only the hysteretic case masquerades as linear [1].

Comparing figures 4 and 5, one observes that the oscillating cube is closest to the case of Coulomb damping. Although one normally associates Coulomb damping with sliding surfaces, we see that it is also a first approximation to the rolling friction of the present study. Because the turning points of the motion deviate from a line (or other simple curve) a non-traditional method of measuring the damping was employed.

5.3 Short Time Fourier Transform

The left set of curves in figure 5 may be familiar to the reader, but the middle set of curves is less common. Because the decay curves of this study are not simple, the method selected for measuring the damping is one called the short time Fourier transform (STFT). The time-record is analyzed, using the Fast Fourier transform (FFT), by evaluating at each of a set of points that are equally spaced in time, and which cover the full span of the record. For a given length record, the maximum allowable number of STFT points is determined by the Δt between points and the number of points used in calculating the FFT. The value of Δt is governed by the sample rate of the ADC and the total duration of the

decay. For all present work the sample rate was 240 s^{-1} . For most of the graphs the time between FFT points was 5.2 s, a value made convenient by the modulus operandus of the Dataq software. Also for the present work, the number of points chosen for each FFT calculation was 1024. Spectra calculated with anything smaller (including 512) yield too poor resolution to be acceptable. For high-level decays with small damping this permitted more than 30 points to be plotted. At low-levels the number was reduced by a factor of about two for small damping cases. When the damping was large, due to surface contamination, the Q was so small as to disallow an accurate assessment of the damping history and thus the mechanism (too few points). From a given spectrum, the level of the fundamental component was read in decibels; this value was then plotted in time at the midpoint of the 1024 point-spread.

As seen from figure 5 (middle graphs), such an STFT yields a straight line if it was obtained from an exponential (hysteretic) decay. If the decay curve derives from Coulomb friction, the STFT curve falls at an ever increasing rate, becoming precipitous at the end time. For amplitude dependent damping (such as from drag of a fluid that is quadratic in the speed), the opposite trend is found.

5.4 Quality Factor

The quality factor in free-decay is defined according to

$$Q = 2\pi \frac{E}{|\Delta E|} \quad (7)$$

where E is the energy of the oscillator at a given time, and $|\Delta E|$ is the energy loss to the damping friction per cycle at that time. For the case of hysteretic damping Q is constant, as observed in the right set of graphs of figure 5. The exponential decay requires of the amplitude A that $\Delta A/A = \text{constant}$, giving $Q = \text{constant}$, since $E \propto A^2$.

The Q of Coulomb damping decreases linearly in time as shown in the graph. This can be easily understood, since the friction force is constant, and the work done against friction is thus proportional to the amplitude. Noting again that the energy is proportional to the square of the amplitude, the Q for this case must then be proportional to the amplitude, which itself falls off linearly. To calculate the Q from the falloff slope in dB/s , one uses the expression $Q = 27.29 \frac{f}{|dB/s|}$, where f is the frequency of oscillation.

A thorough quantitative treatment of these nonlinear damping mechanisms, including the amplitude dependent case, can be found in [1].

6 Damping Measurements

Shown in figure 6 are graphs of STFT and Q vs time for the left case of figure 4. The history of Q is remarkable in its non-classical properties. There are three separate regions of essentially constant slope, implying a different constant 'coefficient' of (internal) friction for each of the three regions. These have been identified by the straight line (red) fits to those segments. The most striking feature of the graph is the peak which occurs at 36 s. Both to the left and to the right of this peak the slope is the same 8.0 s^{-1} . At 68 s, the slope changes discontinuously to the final segment value of 2.1 s^{-1} .

These characteristics were found to be essentially reproducible, as can be seen from figure 7; although the sharpness of the peak is more pronounced in figure 7. If the STFT step-size had been smaller, to improve resolution; perhaps these would be more similar. Although the peak in figure 7 occurs a little later at 42 s, it has roughly the same amplitude of 52 db, corresponding to an energy of $0.2 \mu J$. Either side of the peak in figure 7 the slope is the same 7.0 s^{-1} , whereas the ending (third-segment) slope is 2.6 s^{-1} .

7 Energy Transition

For Coulomb damping $\frac{d\Delta E}{dt} = R$ where R is a negative constant in the absence of any change to the damping. The discontinuous change in the slope of Q that occurs toward the end of the record, in each

of figures 6 and 7, corresponds to a downward jump in the rate at which energy is lost per cycle. If we designate the magnitude of this change in energy rate by $|\delta(R)|$, then from the definition of Q one obtains

$$|\delta(R)| = \frac{2\pi E_0}{Q_0^2} |\delta(\dot{Q})| \quad (8)$$

where the subscript 0 on E and Q identify their values at the time of the change. From the level of the voltage in dB at this point, and using the calibration constant of $48V/rad$, the amplitude was estimated at $\theta_0 = 0.56 \text{ mrad}$ in figure 6. Also at this transition, $Q_0 = 76$. From eq(3) the energy is found to be $E_0 = \frac{mq}{2}(r-a)\theta_0^2$, which yields $E_0 = 9.3 \times 10^{-9} J$, upon substituting the parameter values specified earlier. From the slope change (estimated using trendline fits to each of the segments), $|\delta(\dot{Q})| = 5.6 \text{ s}^{-1}$; and so finally, one obtains an estimate for the energy jump in the rate of $|\delta(R)| = 5.7 \times 10^{-11} J/s$. Multiplying this rate by the period $T = 0.45 \text{ s}$ yields, for the energy jump that occurred at the transition $\Delta\epsilon = 2.6 \times 10^{-11} J$. Repeating the process for figure 7 yielded the value $2.2 \times 10^{-11} J$. Their average at

$$\Delta\epsilon_{est} = 2.4 \times 10^{-11} J \quad (9)$$

is noteworthy.

8 Mesoscale Quantization

The estimated energy transition indicated in eq(9) is tantalizingly close to the ‘hysteron’ postulated by Erber and Peters[1], having the value

$$\Delta\epsilon_h = \frac{mc^2}{\alpha} = 1.01 \times 10^{-11} J \quad (10)$$

where mc^2 is the rest energy of the electron and α is the fine structure constant.

9 Self-organized Stability (SOS)

A well-known fairly recent theory that applies to granular systems is ‘self-organized criticality’ (SOC) [3]. Internal friction damping in a mechanical oscillator is postulated to involve SOC.

The present author has postulated that creep, as with SOC, is at the heart of internal friction damping of mechanical oscillators[4]. During creep, structural members of an oscillator evolve toward metastable states. Thus it appears that ‘self-organized stability’ (SOS) is a process that is likely to exist in the ‘sea’ of SOC. The probability of an SOS process being observable is expected to generally increase as the energy of oscillation decreases.

It is postulated that the peaks in figures 6 and 7 are examples of SOS. Where the Q reaches its highest level, the energy decrement per cycle has decreased to $|\Delta E| \approx 5 \times 10^{-10} J$. Either side of the peak the decrement is larger by roughly a factor of two. Damping involves defect structures. To decrease the energy decrement is to decrease the number of defects operating collectively. In other words, to pass through a peak is to undergo a self-organized stability process that exists in transient form; i.e., a metastable state whose lifetime we here quantify by the half-width of the SOS structure. In figures 6 and 7 this is seen to be of the order of 5 s.

10 High-level Oscillation

Reproducibility of SOS is observed by comparing figures 8 and 9, but there is no evidence for discrete energy transitions as in figures 6 and 7. This is in keeping with the earlier postulate that the transitions are more observable at low energies. Scatter (noise) in figures 8 and 9 is too large to permit their observation. Observe also, that the half-life of the SOS is roughly twice that of the lower energy cases; i.e., now about 10 s.

This author has held to the position for years now, that damping friction is quantized at the mesoscale. Evidence for his position has been found in a variety of largely different experiments, the

first of which involved a low-frequency physical pendulum[5]. Another example, involving a torsion pendulum, is described in an appendix of [1].

It is assumed that dissipation of energy involves the removal of energy ‘packets’ from the oscillator that are integer multiples of the hysteron energy given in eq(10). Whether the decay is hysteretic (exponential) as in earlier experiments, or Coulomb in character (present experiment); at larger energies of oscillation, the discrete nature of the damping is not discoverable in the presence of noise.

11 Surface Contamination

The dramatic influence on damping of the surface state of cube and cylinder is illustrated in figure 11. Prior to the generation of the free-decay record shown, both surfaces were touched with a finger of the hand several times and in several places, in the vicinity of the equilibrium contact point. The fingerprints left on the surfaces resulted in (i) a dramatic reduction in the Q, and (ii) a near perfect example of Coulomb damping throughout the entire record.

Similar records that are not shown, generated after applying various fluids to the surfaces, also resulted in behavior similar to figure 11. Of the three fluids considered for cleaning the surfaces: (i) alcohol, (ii) a computer monitor cleanser, and (iii) acetone; the monitor solvent of unknown chemical composition caused enormous Q reduction, and acetone resulted in the lowest dissipation. The data of figures 3 & 6 - 10 were all obtained after acetone cleaning, followed by half a dozen decay runs before the start of data collection. The reason for the half-dozen pre-data ‘conditioning’ is that the decay curves were found to evolve significantly with time through the first several runs following the application of the acetone.

References

- [1] R. D. Peters, “Damping Theory”, Ch. 20, *Vibration and Shock Handbook*, ed. Clarence deSilva, CRC Press (2005).
- [2] U.S. Patent No. 5,461,319. Online information may be found at <http://physics.mercer.edu/petepag/sens.htm>
- [3] P. Bak, C. Tang, & K. Wiesenfeld, “Self-organized criticality, An explanation of 1/f noise”, *Phys. Rev. Lett.* 59, 381-384 (1987). Also, same authors, *Phys. Rev. A* 38, 364-374 (1988), and *Geophys. Res.* 94, 15,635-15,637 (1989).
- [4] Peters, “Creep and mechanical oscillator damping”, online at <http://arxiv.org/html/physics/0109067>.
- [5] R. Peters, “Metastable states of a low-frequency mesodynamic pendulum”, *Appl. Phys. Lett.* 57, 1825 (1990).

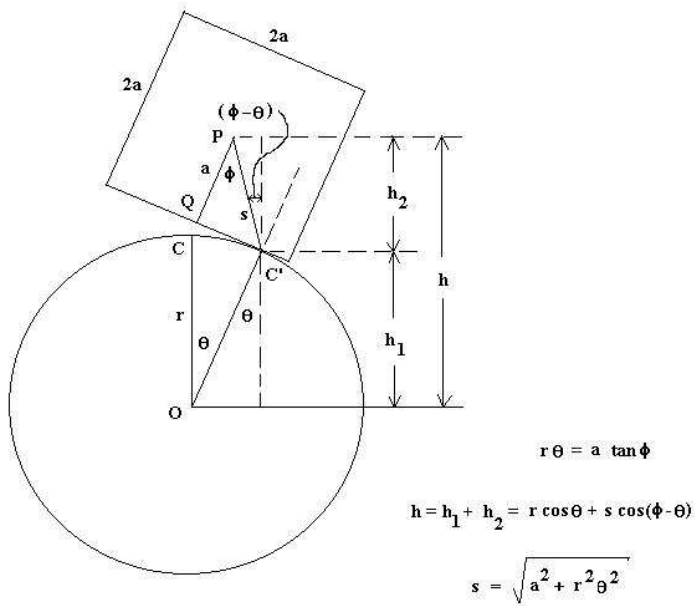


Figure 1: Illustration of the geometry of a cube oscillating on a cylinder.

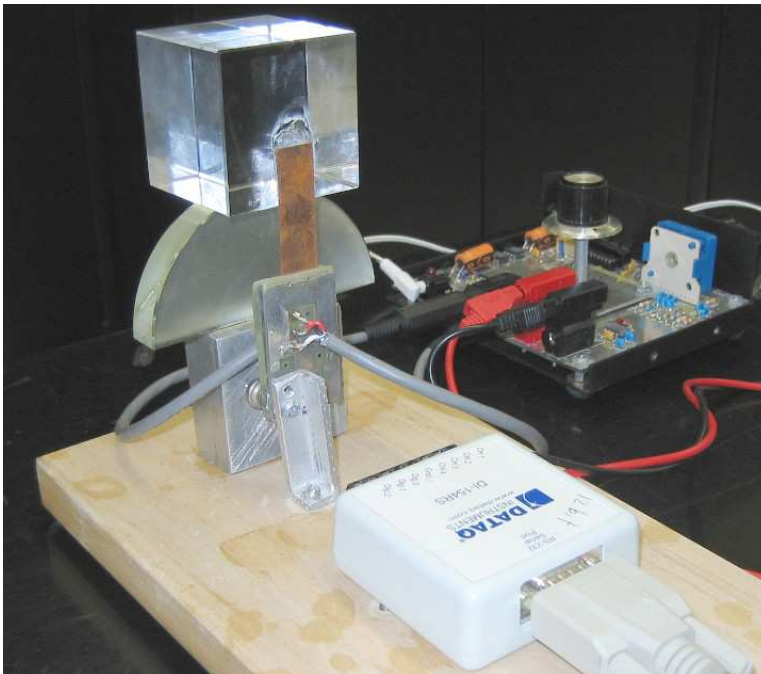


Figure 2: Photograph of the apparatus, showing oscillator, sensor/electronics, and ADC.

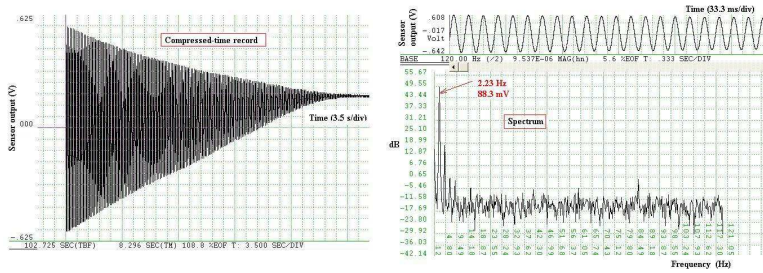


Figure 3: Low-level free-decay record and its spectrum.

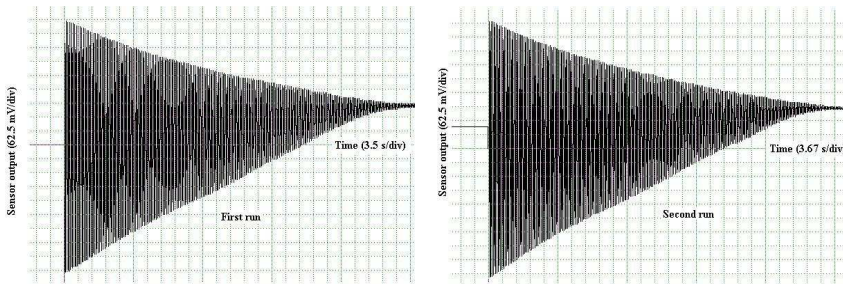


Figure 4: Comparison of two low-level free-decay curves showing a high level of reproducibility.

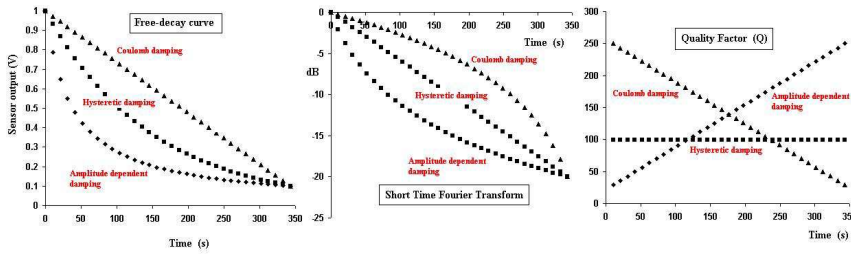


Figure 5: Theoretical curves for three common forms of damping.

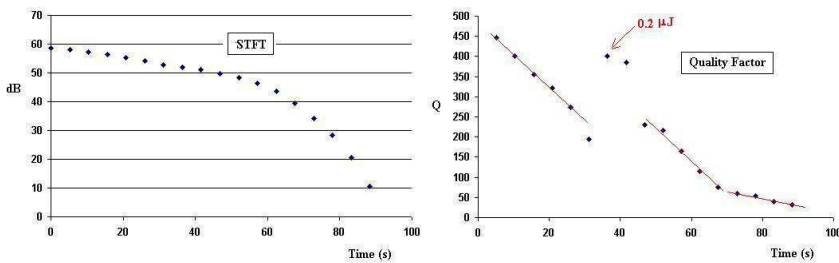


Figure 6: STFT (left) from which the history of Q is obtained (right) –corresponding to left graph of fig. 4.

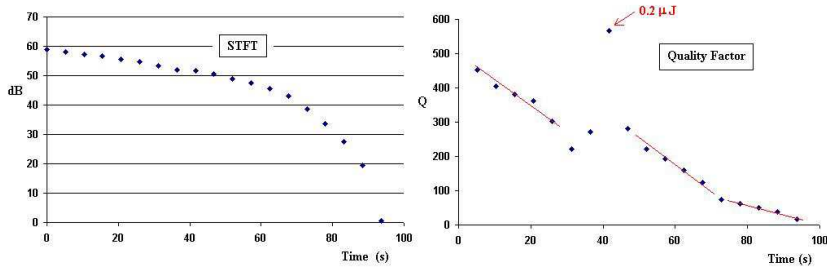


Figure 7: Same as fig. 6, except corresponding to right graph of fig. 4.

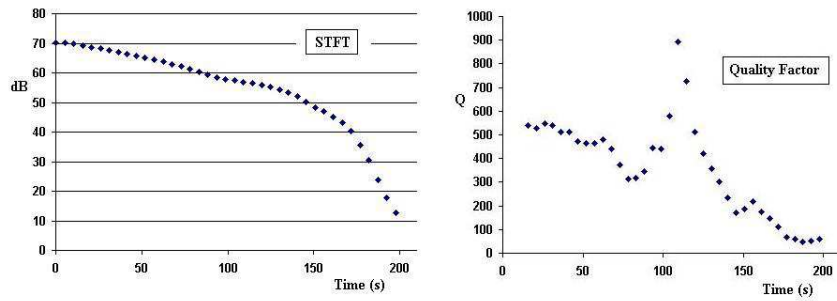


Figure 8: STFT and Q histories for a free-decay at higher starting energy.

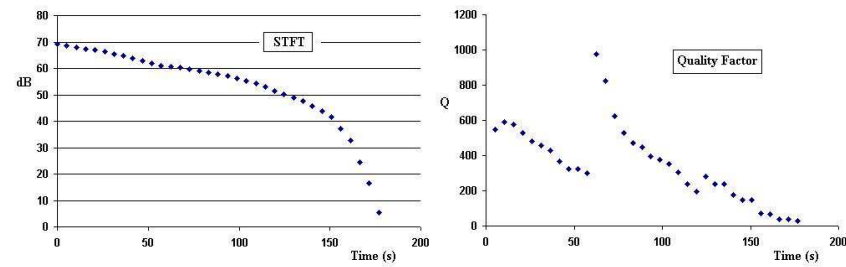


Figure 9: Repeat of figure 8 case, showing reproducibility of SOS.

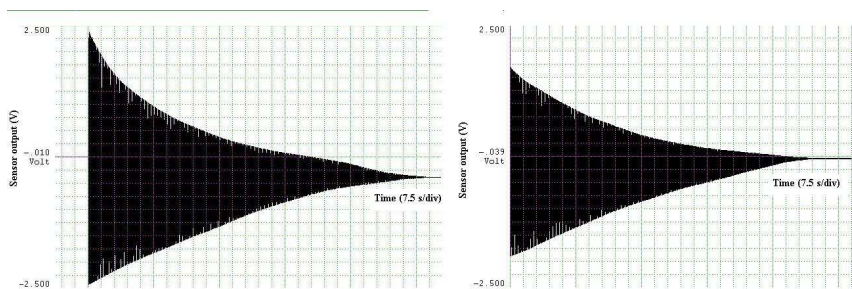


Figure 10: Free-decay records used to generate figures 8 (left) and 9 (right).

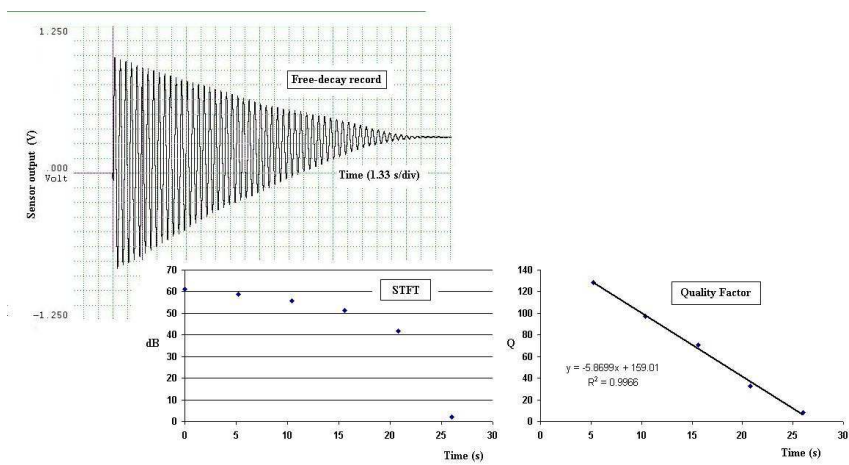


Figure 11: Illustration of the influence of surface contamination.